

A new class of electrically tunable metamaterial terahertz modulators

Rusen Yan,^{1,2} Berardi Sensale-Rodriguez,^{1,2} Lei Liu,¹ Debdeep Jena,¹
and Huili Grace Xing^{1,*}

¹ Department of Electrical Engineering, University of Notre Dame, Notre Dame, IN 46556, USA

² These authors contribute equally to this work

*hxing@nd.edu

Abstract: Switchable metamaterials offer unique solutions for efficiently manipulating electromagnetic waves, particularly for terahertz waves, which has been difficult since naturally occurring materials rarely respond to terahertz frequencies controllably. However, few terahertz modulators demonstrated to date exhibit simultaneously low attenuation and high modulation depth. In this letter we propose a new class of electrically-tunable terahertz metamaterial modulators employing metallic frequency-selective-surfaces (FSS) in conjunction with capacitively-tunable layers of electrons, promising near 100% modulation depth and < 15% attenuation. The fundamental departure in our design from the prior art is tuning enabled by self-gated electron layers that is independent from the metallic FSS. Our proposal is applicable to all possible electrically tunable elements including graphene, Si, MoS₂, oxides etc, thus opening up myriad opportunities for realizing high performance switchable metamaterials over an ultra-wide terahertz frequency range.

©2012 Optical Society of America

OCIS codes: (250.4110) Modulators; (160.3918) Metamaterials; (040.2235) Far infrared or terahertz.

References and links

1. A. D. Boardman, V. V. Grimalsky, Y. S. Kivshar, S. V. Koshevaya, M. Lapine, N. M. Litchinitser, V. N. Malnev, M. Noginov, Y. G. Rapoport, and V. M. Shalaev, "Active and tunable metamaterials," *Laser Photon. Rev.* **5**(2), 287–307 (2011).
2. M. Tonouchi, "Cutting-edge terahertz technology," *Nat. Photonics* **1**(2), 97–105 (2007).
3. H. T. Chen, W. J. Padilla, J. M. O. Zide, A. C. Gossard, A. J. Taylor, and R. D. Averitt, "Active terahertz metamaterial devices," *Nature* **444**(7119), 597–600 (2006).
4. T. Kleine-Ostmann, P. Dawson, K. Pierz, G. Hein, and M. Koch, "Room-temperature operation of an electrically driven terahertz modulator," *Appl. Phys. Lett.* **84**(18), 3555–3557 (2004).
5. T. Kleine-Ostmann, K. Pierz, G. Hein, P. Dawson, M. Marso, and M. Koch, "Spatially resolved measurements of depletion properties of large gate two-dimensional electron gas semiconductor terahertz modulators," *J. Appl. Phys.* **105**(9), 093707 (2009).
6. B. Sensale-Rodriguez, T. Fang, R. Yan, M. M. Kelly, D. Jena, L. Liu, and H. G. Xing, "Unique prospects for graphene-based terahertz modulators," *Appl. Phys. Lett.* **99**, 113104 (2011).
7. B. Sensale-Rodriguez, R. Yan, M. M. Kelly, T. Fang, K. Tahy, W. S. Hwang, D. Jena, L. Liu, and H. G. Xing, "Broadband graphene terahertz modulators enabled by intraband transitions," *Nat Commun* **3**, 780 (2012).
8. B. Sensale-Rodriguez, R. Yan, S. Rafique, M. Zhu, W. Li, X. Liang, D. Gundlach, V. Protasenko, M. M. Kelly, D. Jena, L. Liu, and H. G. Xing, "Extraordinary control of terahertz beam reflectance in graphene electro-absorption modulators," *Nano Lett.* **12**(9), 4518–4522 (2012).
9. F. Xia, T. Mueller, R. Golizadeh-Mojarad, M. Freitag, Y. M. Lin, J. Tsang, V. Perebeinos, and P. Avouris, "Photocurrent imaging and efficient photon detection in a graphene transistor," *Nano Lett.* **9**(3), 1039–1044 (2009).
10. Z. Sun, T. Hasan, F. Torrisi, D. Popa, G. Privitera, F. Wang, F. Bonaccorso, D. M. Basko, and A. C. Ferrari, "Graphene mode-locked ultrafast laser," *ACS Nano* **4**(2), 803–810 (2010).
11. R. Yan, Q. Zhang, W. Li, I. Calizo, T. Shen, C. A. Richter, A. R. Hight-Walker, X. Liang, A. Seabaugh, D. Jena, H. G. Xing, D. J. Gundlach, and N. V. Nguyen, "Determination of graphene work function and graphene-insulator-semiconductor band alignment by internal photoemission spectroscopy," *Appl. Phys. Lett.* **101**(2), 022105 (2012).
12. K. F. Mak, M. Y. Sfeir, Y. Wu, C. H. Lui, J. A. Misewich, and T. F. Heinz, "Measurement of the Optical Conductivity of Graphene," *Phys. Rev. Lett.* **101**(19), 196405 (2008).

13. B. Sensale-Rodriguez, R. Yan, S. Rafique, M. Zhu, V. Protasenko, D. Jena, L. Liu, and H. G. Xing, "Exceptional Tunability of THz Reflectance in Graphene Structures", IRMMWTHz 2012, Wollongong, Australia, 2012.
14. H. T. Chen, W. J. Padilla, M. J. Cich, A. K. Azad, R. D. Averitt, and A. J. Taylor, "A metamaterial solid-state terahertz phase modulator," *Nat. Photonics* **3**(3), 148–151 (2009).
15. P. Tassin, T. Koschny, M. Kafesaki, and C. M. Soukoulis, "A comparison of graphene, superconductors and metals as conductors for metamaterials and plasmonics," *Nat. Photonics* **6**(4), 259–264 (2012).
16. B. Radisavljevic, A. Radenovic, J. Brivio, V. Giacometti, and A. Kis, "Single-layer MoS₂ transistors," *Nat. Nanotechnol.* **6**(3), 147–150 (2011).
17. K. F. Mak, C. Lee, J. Hone, J. Shan, and T. F. Heinz, "Atomically thin MoS₂: a new direct-gap semiconductor," *Phys. Rev. Lett.* **105**(13), 136805 (2010).
18. W. S. Hwang, M. Remskar, R. Yan, V. Protasenko, K. Tahy, S. D. Chae, P. Zhao, A. Konar, H. G. Xing, A. Seabaugh, and D. Jena, "Transistors with chemically synthesized layered semiconductor WS₂ exhibiting 105 room temperature modulation and ambipolar behavior," *Appl. Phys. Lett.* **101**, 013107 (2012).
19. S. Kim, A. Konar, W. S. Hwang, J. H. Lee, J. Lee, J. Yang, C. Jung, H. Kim, J. B. Yoo, J. Y. Choi, Y. W. Jin, S. Y. Lee, D. Jena, W. Choi, and K. Kim, "High-mobility and low-power thin-film transistors based on multilayer MoS₂ crystals," *Nat Commun* **3**, 1011 (2012).
20. S. J. Allen, D. C. Tsui, and R. A. Logan, "Observation of the two-dimensional plasmon in silicon inversion layers," *Phys. Rev. Lett.* **38**(17), 980–983 (1977).
21. Y. W. Tan, Y. Zhang, K. Bolotin, Y. Zhao, S. Adam, E. H. Hwang, S. Das Sarma, H. L. Stormer, and P. Kim, "Measurement of scattering rate and minimum conductivity in graphene," *Phys. Rev. Lett.* **99**(24), 246803 (2007).

1. Introduction

Over the past decades the terahertz frequency regime (0.1–30 THz) has become the subject of much attention due to its important applications in astronomy, imaging, spectroscopy, etc [1–3]. At present, development of components to efficiently control and manipulate THz waves is still lagging behind. For instance, in 2004 Kleine-Ostmann et al. proposed a semiconductor structure consisting of a metal-gated two-dimensional-electron-gas (2DEG) to modulate the intensity of terahertz waves for broadband operation at room temperature, but the experimental results showed high insertion loss (~90% intensity loss) and poor modulation depths (~6%) [4,5]. Alternatively, THz modulators based on metamaterials have showed great potential due to their good performance in terms of modulation depth and attenuation loss. Recently our group have proposed and experimentally demonstrated a graphene-based THz amplitude modulators with a low insertion loss of 5% [6,7]. However, all the attempts reported to date exhibit unavoidable trade-offs between modulation depth, signal attenuation loss, polarization dependence, ease of fabrication and design flexibility. In this work, we propose a new class of electrically tunable metamaterials consisting of capacitively-coupled layers of electrons that are structurally complementary to, but, only electromagnetically connected with the metallic frequency selective surface (FSS) structures. In the previously reported tunable metamaterials, the tunable elements are also electrically controlled by the metallic FSS, which limits its design freedom thus modulator performance. Our proposed devices allow one to construct tunable metamaterials by placing the self-gated electron layers at optimal locations relative to the metallic FSS. This simple but elegant solution enables remarkably low insertion loss and high modulation depth, simultaneously. We also emphasize that the methodology described in this letter can be readily extended to other switchable metamaterials designs as well as other electrically tunable materials including conventional semiconductors, transition metal oxides and so on.

2. Proposed device structure

Below, to illustrate the key design strategy in constructing switchable metamaterials operating as THz intensity modulators, we use a pair of graphene sheets as example self-gated electron

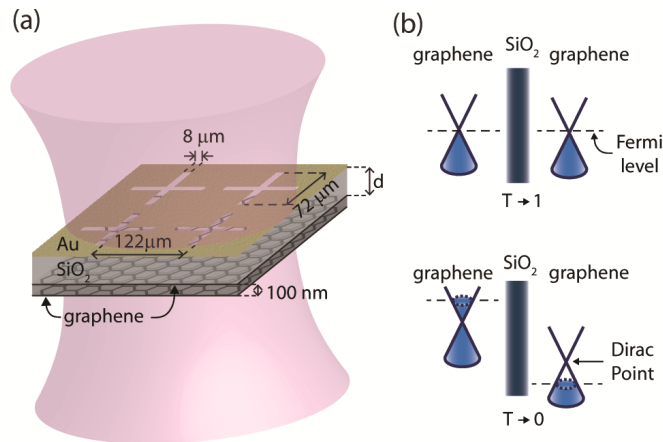


Fig. 1. An example of the proposed new class of electrically tunable metamaterial THz modulators. a) The proposed THz modulator structure consists of a square lattice of gold cross-slot FSS and a pair of capacitively-coupled graphene layers situated at a distance d . The dielectric separating the FSS and graphene pair and between graphene layers is assumed to be SiO_2 . The other dimensions used in simulation are shown in the graph. b) Energy band diagrams of the graphene pair. At zero bias, the Fermi level is at the Dirac point of both graphene layers, leading to minimum conductivity and maximum terahertz transmission at the resonant frequency. When biased, the Fermi level moves into the conduction and valence band of the two graphene layers, respectively, resulting in an enhanced conductivity and minimized terahertz transmission.

layers and a square lattice of gold cross-slots as an example metallic FSS, as shown in Fig. 1(a). Graphene is chosen since it enables facile fabrication of the proposed modulators and allows us to compare the proposed device with the existing ones based on graphene [7]. In addition, graphene, emerging as an attractive material candidate for future optics and electronics, has been proposed and demonstrated with exciting potentials in diverse applications including transparent contacts, photodetectors, ultra-fast lasers and optical modulators [7–11]. Absorption by graphene in the infrared and visible range is only about 2.3% at normal incidence, which is limited by the interband transitions, i.e. an electron in the valence band absorbs a photon and gets excited to the conduction band [12]. However, in the THz range the atomically thick graphene can potentially absorb up to 100% of the incident THz photons since this physical process is determined by the intraband transitions, i.e. an electron absorbs a THz photon with an energy on the order of meV and stays in the same energy band. In our previous work, we have shown in details that in a transmission mode, a single layer graphene can absorb up to 50% of the THz photons when its conductivity is tuned to be ~ 5 mS [6,7]; and that in a reflection mode, graphene can absorb up to 100% when its conductivity is tuned to be ~ 2.7 mS [8,13]. The experimentally demonstrated THz absorption by graphene to date has reached $> 50\%$ [8], which is limited by the typical quality of the state-of-the-art large-area graphene.

In the modulator proposed here, the gold-mesh FSS behaves as a band-pass electromagnetic field concentrator; the band-pass center frequency (f_0) and bandwidth (Δf) are determined by the mesh grid dimensions, the degree of in-plane field concentration is determined by the distance d . The graphene pair positioned in the concentrated in-plane field region at d plays a role of modulating the amplitude of the transmitted terahertz waves [6,7]. The dielectric separating the FSS and the graphene pair as well as that between the two graphene layers is assumed to be SiO_2 . The energy band diagrams of this graphene pair are shown in Fig. 1(b). Transmission of THz waves reaches maximum when the Fermi levels in the graphene pair are at the Dirac point due to minimized intraband and interband transitions in graphene; it decreases as Fermi levels are tuned away from Dirac point due to increasing intraband transitions [6,7]. Considering the symmetric band structure of graphene around its

Dirac point, we can assume the electrical thus optical conductivity of the two graphene layers to be the same. Therefore, the conductivity value assumed in all the figures in this letter is that of a single graphene layer or half of the total conductivity of the 2DEG-pair.

3. Simulation results and analysis

To obtain terahertz transmission properties, the two port S parameters of the modulators in Fig. 1(a) were simulated using a finite element based 3D electromagnetic solver: high frequency structure simulator (HFSS) by ANSYS, Inc. In Fig. 2(a) and 2(b) the amplitude of both S_{21} (transmittance) and S_{11} (reflectance) are plotted as a function of half of the 2DEG-pair conductivity, for $d = 10 \mu\text{m}$. The terahertz wave absorption by the metamaterial modulator can be extracted accordingly and is shown in Fig. 2(c). With increasing graphene conductivity, both reflection and absorption in the 2DEG-pair increase, leading to a decrease of transmission. For a moderate conductivity swing of 0.001 – 2 mS per 2DEG layer, the transmittance can be tuned in a large range while the resonant frequency does not shift. At very high conductivities, e.g. 5 mS per 2DEG layer, the absorption tends to decrease because of the increasing reflection. The maximum absorption by the 2DEG-pair is about 50%, consistent with what we discovered in broadband graphene terahertz modulators [7]. The phase of transmittance is plotted in Fig. 2(d), and it is observed that the phase change with the 2DEG conductivity is negligible at the resonant frequency except at very high conductivities. In fact, significant phase change occurs at lower conductivities when the 2DEG pair is placed closer to the metallic FSS (not shown). This effect was explored to realize broadband modulation using field-sensitive detection (e.g. time domain THz spectroscopy) in a metamaterial design where metallic FSS sits right on top of the semiconductor thus the phase change is most sensitive to the conductivity [14].

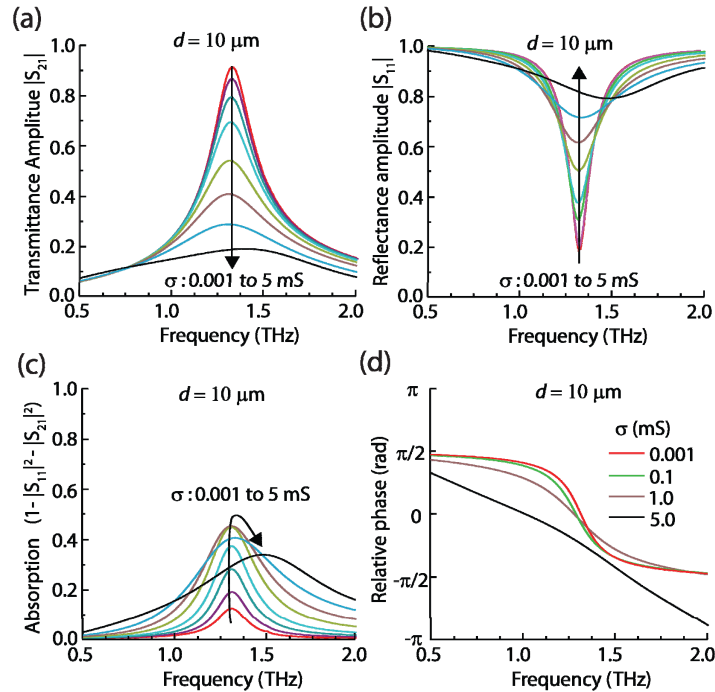


Fig. 2. The simulated behavior of the example modulator shown in Fig. 1 as a function of half of the 2DEG-pair conductivity. (a) Transmittance (S_{21}) amplitude, (b) reflectance (S_{11}) amplitude, (c) associated absorption by the modulator, and (d) phase of transmittance. With increasing 2DEG-pair conductivity, both absorption in the 2DEG-pair and reflection by the modulator increase. At very high conductivities (e.g. 5mS), a shift in resonant frequency is observed, resulting in accompanied higher reflection, reduced absorption and augmented phase shift. There is negligible phase change at the resonant frequency except at very high conductivities.

In Fig. 3(a), the power transmittance of the proposed modulator at the resonance frequency as a function of half of the 2DEG-pair conductivity are plotted with varied separating distance d between the FSS and 2DEG-pair. The red, pink and green curves correspond to different placements of the 2DEG-pair, $d = 1, 5, 10 \mu\text{m}$. The black curve (analytical results [6,7]) and blue circle points (HFSS simulation results) in Fig. 3 correspond to the intensity transmittance through a pair of graphene suspended in air, which match with each other. This excellent agreement of analytical and HFSS solutions demonstrate the validity of our modeling approach. For a given 2DEG-pair conductivity, the closer it is placed to the metallic FSS, the lower the intensity transmittance due to stronger near-field effects or concentrated field in the 2DEG planes. For a 2DEG-pair conductivity of $2 \times 0.001 \text{ mS}$, the amplitude transmittance reaches near 91%, i.e. an intensity insertion loss of $1 - 0.91^2 \sim 17\%$. More careful examination revealed that the finite conductivity of gold [15] ($2 \times 10^{-6} \text{ Ohm-cm}$) and the 2DEG-pair results in absorption of 12% and 2%, respectively; and the rest of the intensity insertion loss (3%) is due to the reflection of the metamaterial stemming from the substrate refractive index and thickness [7]. When the 2DEG-pair conductivity increases to $2 \times 5 \text{ mS}$, the amplitude transmittance is $< 20\%$; this corresponds to a modulation depth of the amplitude transmittance: $(91-20)/91 \sim 78\%$, or of the intensity transmittance: $(91^2-20^2)/91^2 \sim 95\%$. The pink shaded region in Fig. 3(a) marks the typical tunable conductivity range of a single-layer graphene. For $d = 10 \mu\text{m}$ and the typical conductivity tunable range of a single-layer graphene, the resultant intensity modulation depth is about $(62-16)/62 \sim 74\%$ with an insertion loss of $\sim 38\%$. The improvement in modulation depth over that achievable by a suspended graphene pair without a field enhancing architecture is appreciable, which is $\sim 42\%$, although the suspended pair offers broadband operation with a lower insertion loss of $\sim 9\%$ [7]. When a graphene pair is placed at $d = 1 \mu\text{m}$, the resultant intensity modulation depth is about $(14-2)/14 \sim 86\%$ with an insertion loss of 86%.

A high modulation depth is attractive; however, too close a placement is not desirable since it introduces an extremely high insertion loss. The tradeoff between modulation depth and insertion loss is shown in Fig. 3(b) for two tunable conductivity ranges: $0.1 - 1 \text{ mS}$ and $0.001 - 1 \text{ mS}$. Also shown are two representative experimental results [3,7], suggesting that superior performance can be achieved with proper choices of the tunable materials. A wide conductivity range with a lower minimum conductivity gives rise to the desired modulation performance: low insertion loss and high modulation depth. Although graphene is promising in constructing the proposed electrically tunable terahertz modulator due to its facile integration with other materials and low cost in large-scale production, its minimum conductivity due to the zero bandgap can introduce an appreciable insertion loss. To further improve the modulator performance, it is necessary to adopt other tunable elements with lower optical conductivities for the terahertz frequency range of interest. In this regard, Si becomes a strong contender among all possible candidates due to its maturity. One can potentially use a thin membrane of Si/SiO₂/Si as the self-gated electron layers. The major advantage of the Si-Si pair is that its conductivity can be tuned to be below 10^{-5} mS , where absorption by mobile electrons is practically zero. Considering a moderate conductivity range of $10^{-5} - 0.5 \text{ mS}$, one can see from Fig. 3(a) that a near unity modulation depth with an insertion loss of $< 15\%$ can be obtained. One can also stack multiple tunable elements to enhance modulation depth with a limited range of tunable conductivity as long as they do not introduce excessive insertion loss. It is also conceived that those structures can be readily fabricated employing 2D semiconductor crystals with non-zero bandgap, such as MoS₂ and WS₂ [16–19], for their easy integration and low minimum conductivity.

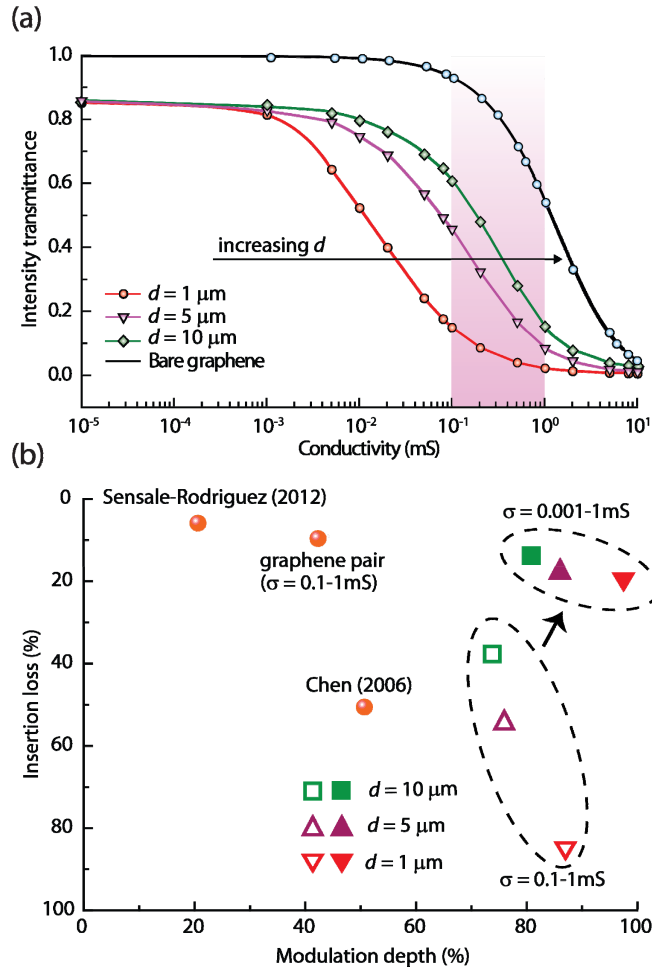


Fig. 3. a) Intensity transmittance at the resonant frequency versus the half conductivity of the 2DEG-pair at different separating distance between the pair and metamaterials. The red, pink and green curves correspond to $d = 1, 5, 10 \mu\text{m}$. The black curve and blue circles points are, respectively, analytical solutions [7] and HFSS simulation results corresponding to the intensity transmittance through a pair of graphene suspended in air. The pink shaded region shows the typical range of single-layer graphene conductivity. b) Tradeoffs between insertion loss and modulation depth extracted from Fig. 3(a) for two ranges: $\sigma = 0.1-1 \text{ mS}$ and $0.001-1\text{mS}$.

4. Near-field effects and THz frequency range considerations

Indeed, by placing the electron layers in a cavity, their absorbance/reflectance at a given conductivity can be augmented. To better understand the physical picture for the enhanced modulation, we plot in Fig. 4 the Poynting vector distribution in the cross sectional plane of the metallic FSS alone cut along the centerline of the cross. The FSS plane is denoted as $z = 0 \mu\text{m}$ and the incident wave propagates along the $+z$ direction. Near the center of the cross, the magnitude of the Poynting vector distribution is strongest given the electromagnetic wave cannot penetrate gold thus funnel through the cross opening. Far away from the FSS ($z > 50 \mu\text{m}$), it shows a plane wave propagating along $+z$ direction with rather uniformly distributed intensity. Furthermore, near the metal FSS, the electromagnetic wave largely propagates in the x-y plane, which leads to a dramatically augmented propagation length in the 2DEG layers when it is placed close to the FSS. The combination of enhanced field strength and in-

plane propagation length in the near field of the FSS results in enhanced absorption thus exceptional modulation by the 2DEG layers when placed close.

Finally we discuss the operation frequency range of the proposed switchable terahertz metamaterials enabled by the self-gated electron layers. The optical conductivity of mobile electrons in the terahertz to infrared region (below photon energies that trigger interband transitions) is determined by their Drude and plasmonic behavior. For simplicity, let us consider the Drude conductivity only: it decreases with increasing frequency. For instance, the Drude dominated terahertz bandwidth in graphene has been found to be near 4 THz [7,20]. As a result, we can assume that the graphene optical and DC electrical conductivities are the same in the above example device designed near 1.3 THz. Another advantage of the proposed device in this letter is that it allows the location of the self-gated electron layers to be optimized depending on their tunable conductivity range at the designed terahertz frequency. For a graphene-based device operating at a frequency band < 4 THz, the optimal location is near $d = 10 \mu\text{m}$ for the example design; while for a device operating at a band near 10 THz, the optimal location could be near $d = 1 \mu\text{m}$. It is also straightforward to extend similar design considerations to devices employing tunable plasmonic effects, which play important roles above the Drude dominated frequency range [20,21]. We also like to point out that our discussions focus on tunable elements, including graphene and other materials with tunable optical conductivity in the terahertz band, while the primary frequency selective features in the switchable metamaterials should be made of low-loss materials such as gold [15], silver [15] or dielectric cavities to minimize the device insertion loss.

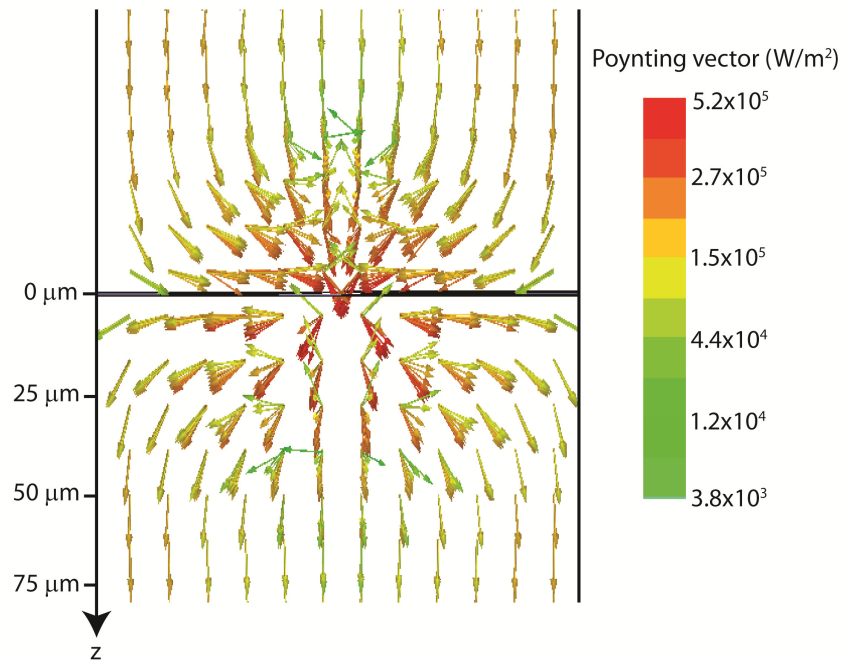


Fig. 4. Cross sectional Poynting vector distribution near the metallic FSS along cut along the centerline of the cross. The FSS lies at the $z = 0 \mu\text{m}$ plane. The color and direction of the arrows indicate the amplitude and propagation direction of the THz wave, respectively.

5. Conclusion

We have proposed a new class of metamaterial-based tunable THz modulators with significant improvements in modulation depth, insertion loss, fabrication, integration and design flexibility. Our simple but unique idea ensures that the amplitude-modulating 2DEG-pair work independently with frequency-selective metamaterials, thus providing significantly more freedom in the device design. Our proposal can be readily applied into a variety of promising materials, such as graphene, Si, MoS₂, oxides etc, which holds promise for future experimental realization of high-performance tunable THz modulators.

Acknowledgments

Xing acknowledges the support from National Science Foundation (CAREER, monitored by Anupama Kaul). Jena and Xing acknowledges the support from the Air Force Office of Scientific Research (FA9550-12-1-0257, monitored by James Hwang) and from the Office of Naval Research (N00014-11-1-0721, monitored by Paul Maki and Daniel Green). Liu and Xing acknowledge the support from National Science Foundation (ECCS-1202452, monitored by Samir El-Ghazaly). Liu, Jena and Xing also acknowledge the support from the Center of Advanced Diagnostics & Therapeutics (AD&T), the Midwest Institute of Nanoelectronics Discovery (MIND) and the Center for Nanoscience and Technology (ND nano) at the University of Notre Dame.